



Article

Evaluation of Mango Kernel Seed (*Mangifera indica*) Oil as Cutting Fluid in Turning of AISI 1525 Steel Using the Taguchi-Grey Relation Analysis Approach

Rasaq A. Kazeem¹, David A. Fadare¹, Omolayo M. Ikumapayi^{2,*}, Stephen A. Akinlabi³ and Esther T. Akinlabi^{4,5}

¹ Department of Mechanical Engineering, University of Ibadan, Ibadan 200281, Nigeria; kazeemaddebayo85@yahoo.com (R.A.K.); fadareda@yahoo.com (D.A.F.)

² Department of Mechanical and Mechatronics Engineering, Afe Babalola University, Ado Ekiti 360101, Nigeria

³ Department of Mechanical Engineering, Butterworth Campus, Walter Sisulu University, Mthatha 5117, South Africa; stephenakinlabi@gmail.com

⁴ Department of Mechanical Engineering Science, University of Johannesburg, Auckland Park, Johannesburg 2006, South Africa; etakinlabi@gmail.com

⁵ Pan African University Life and Earth Sciences, Ibadan 200284, Nigeria

* Correspondence: ikumapayi.omolayo@abuad.edu.ng; Tel.: +234-803-078-1881

Abstract: The hunt for environmentally friendly cutting fluids is underway as the problems of conventional cutting fluids become more evident. To achieve environmentally conscious machining, the current study examines the use of Mango Kernel Seed Oil (MKSO) as a cutting fluid during the turning of AISI 1525 steel. According to the 2⁴ complete factorial techniques, the vegetable-oil-based cutting was produced by dissolving four different additives in mango kernel seed oil: emulsifying, antimicrobial, anti-corrosive, and antifoam substances. Afterward, the formulated vegetable oil was characterized both physically and chemically to determine its capability. The developed MKSO was mechanically evaluated using a Taguchi L₉ orthogonal array. Spindle speed, depth of cut, and feed rate served as the input parameters, while surface roughness, cutting temperature, machine sound level, and machine vibration rate were the responses. Taguchi-based Grey Relational Analysis was used to perform multi-objective optimization. It was used to determine the best machining conditions. The best parameters for mango kernel seed oil are a spindle speed of 0.683 rev/min, feed of 0.617 mm/rev, and depth of cut of 0.620 mm, while the optimum parameter for Mineral-Oil-based Cutting Fluid (MOCF) is 0.7898 rev/min spindle speed, 0.6483 mm/rev feed, and a 0.6373 mm depth of cut. This research revealed that, when compared to the feed rate and the depth of cut, the spindle speed has the highest influence on multi-responses in turning operations with both cutting fluids. Generally, MOCF outperformed mango kernel seed cutting fluid in most machining conditions.

Keywords: cutting fluid; grey relational analysis; mango kernel seed oil; mineral oil; Taguchi technique



Citation: Kazeem, R.A.; Fadare, D.A.; Ikumapayi, O.M.; Akinlabi, S.A.; Akinlabi, E.T. Evaluation of Mango Kernel Seed (*Mangifera indica*) Oil as Cutting Fluid in Turning of AISI 1525 Steel Using the Taguchi-Grey Relation Analysis Approach. *Lubricants* **2022**, *10*, 52. <https://doi.org/10.3390/lubricants10040052>

Received: 14 February 2022

Accepted: 11 March 2022

Published: 29 March 2022

Publisher's Note: MDPI stays neutral with regard to jurisdictional claims in published maps and institutional affiliations.



Copyright: © 2022 by the authors. Licensee MDPI, Basel, Switzerland. This article is an open access article distributed under the terms and conditions of the Creative Commons Attribution (CC BY) license (<https://creativecommons.org/licenses/by/4.0/>).

1. Introduction

Machining is a core aspect of manufacturing in engineering. In various engineering tools, machine parts are products of metal machining. Certain parameters are considered when establishing the quality of the final product during the machining process. The cutting fluid used is also an important factor in the finished product's quality. Cutting fluids are used to remove, eliminate, or at least lessen the friction, heat flux effect, and corrosion of both the workpiece and the tool during machining [1]. Several cutting fluids have been made from petroleum products. The petroleum-based cutting fluids are non-biodegradable and highly toxic; therefore, they pose serious threats to the environment and workers' health. When inappropriately discharged, they damage soil and water resources, causing serious environmental impacts. In the workstation, the machine operators may

be affected by health issues, such as skin and respiratory problems. The industry is trying to shift to environmentally friendly, biodegradable oils from vegetable sources. Vegetable oils are more natural, organic, non-toxic, non-polluting, and less expensive. As opposed to MOCFs, different plant oils have different properties owing to their unique chemical properties. Current findings have found that bio-based cutting fluids have greater lubricity and viscosity reduction at elevated temperatures over conventional oil-based cutting fluids [2].

Vegetable oils as cutting fluids have been widely used in several machining operations, such as drilling, milling, turning, and grinding [3]. Vegetable oils often demonstrate very good efficiency as lubricants. Ramana et al. [4] conducted evaluations of surface roughness under three different conditions, e.g., dry, palm oil, palm oil mixture, and boric acid lubricant, during the process of turning Ti-6Al-4V alloy with uncoated tungsten carbide, CVD-coated, and PVD-coated carbide tools. The result showed that palm oil is stronger when applied, compared to dry conditions, and palm oil with boric acid cutting fluids. Singh et al. [5] directed analyses on the capability of mineral and vegetable oils on surface roughness during the turning of EN31 steel under MQL and dry environments. Both MOCF and vegetable oil (soybean) were conveyed as mist MQL targeted at the rake face of the tool at a specific pressure of 5 bar. It was noted that vegetable oil was superior to MOCF as far as surface finish. The decrease of surface roughness owing to vegetable oil was around 1–10%, contrasted with MOCF. Majak et al. [6] considered AISI 304 stainless steel as the processing material in a test to analyze chip compression ratio and surface finish in MQL turning with three kinds of vegetable oils: palm, sunflower, and coconut oils. The general performance of the effectiveness of the cutting oils in decreasing chip compression ratio and improving the surface roughness was better when sunflower oil was applied, as compared to palm and coconut oils. Gunerkar and Kuppan [7] considered an investigation on two distinctive vegetable cutting oils produced from processed sunflower and rapeseed oils, and an industrial mineral machining fluid to establish the least surface roughness, cutting forces, and tool wear during the turning of SS316. Vegetable oils are blended with water in an oil proportion of 1:100. Vegetable oils were discovered to be more beneficial than MOCF when all the yield parameters were considered. Rapeti et al. [8] dealt with the utilization of vegetable oil and a nanoparticle blend as cutting fluids while turning AISI 1040 steel, taking into account eco-friendly machining. Cutting fluids were produced by dissolving nanosuspensions of molybdenum disulfide, MoS₂ in canola, coconut, and sesame oils and were supplied to the cutting area at different cutting conditions, as recommended by L₂₇ Taguchi DOE. It was stated that coconut oil +0.5% nano molybdenum sulfide, when deployed at 0.5% nanoparticle inclusions, 40 m/min cutting speed and 0.14 mm/rev feed rate, enhanced cutting efficiency. According to Shaikh and Sidhu [9], the efficacy of three metalworking fluids (cottonseed, servo cut, and soybean oils) was determined with reference to material removal rates and surface roughness during flood turning operation of AISI D2 steel. The findings indicated that soybean and cottonseed oils should replace servo cut oil due to their user-friendliness, availability, and cost.

Moreover, Kazeem et al. [10] researched the presentation of a vegetable oil that is referred to less frequently—one derived from jatropha—as machining fluid. The jatropha oil was portrayed as having lubricity and phytochemical and physiochemical properties. In turning a low carbon steel alloy, AISI 1525, with a coated carbide tool, the impact of emulsion jatropha oil on machining temperature, chip shape, and surface roughness was tested and compared with MOCF. In most machining environments, jatropha oil achieved better efficiency than MOCF. The Grey relational analysis (GRA) solution showed that the appropriate multi-response efficiency of the industrial MOCF and jatropha oil could be achieved using the same feed rate (0.10 mm/rev) and cutting velocity (355 m/min), but with a DOC of 1.25 and 1.00 mm, respectively. Ojolo et al. [11] investigated the turning of aluminum alloy, copper alloy, and mild steel with a tungsten carbide tool in a wet environment. The impact of four oils, namely shea butter, coconut, palm kernel and groundnut oils, was tested on the force of the cutting process. They observed a better

performance with groundnut oil. Groundnut oil showed the greatest cutting force reduction when aluminum was machined at comparable feed rates and speeds. Bhowmik et al. [12] performed experimental research on the performance of three environmentally friendly oils (groundnut, neem, and soy) and one industrial MOCF oil (supa) in a mild steel turning operation under wet and dry environments. Chip thickness formed using groundnut oil was the highest as compared to the other cutting oils. The viscosity of groundnut oil was the least, and the variation was the closest, even at extreme temperatures. Some other researchers have established in previous research findings that vegetable oils can be used as cutting fluids in turning, drilling, and other metal machining methods and achieve good cooling and lubrication results.

It has been observed that the majority of the vegetable oils used in the literature are edible and may compete with human consumption if promoted, thereby making them more expensive as cutting fluids. Few studies have been done on the applicability of lesser-known vegetable oils as cutting fluids [13]. This study, therefore, aims at investigating the efficiency of a lesser-known vegetable oil (MKSO) as a machining cutting fluid. Based on surface roughness, cutting temperature, machine sound level, and machine vibrations, the developed oil will be mechanically compared to traditional MOCF in the turning of AISI 1525 steel.

2. Methodology

The methodology is divided into two different sections: (i) Collection of seeds, oil extraction and characterization, and formulation of cutting fluids emulsion; and (ii) collection of workpiece materials and cutting tools, determination of physical and chemical properties, and machining trials.

2.1. Seed Samples Description

A mango seed sample was considered in this study. Mango (*Mangifera indica*) is a member of the Anacardiaceae group. Mangos are commonly referred to as the “lord of fruits” in the tropical world; however, after being used or consumed by the mango processing sector, the seeds are usually discarded as garbage [14,15]. Depending on the cultivar, mango seed makes up 35–55 percent of the fruit [16]. The oil portion extracted from mango kernel contains nearly 15% oil [17]. According to research, the mango kernel is a possible future source of a variety of antioxidants and bioactive substances. The cardioprotective and hepatic antioxidant properties of phenolics, as well as their anti-carcinogenic and anti-aging properties, have been proven scientifically for the most part [18]. A prestigious fruit juice company in Ibadan, Nigeria’s southwestern region provided the mango wastes used for the study.

The samples were rinsed, and the core contained within the casing was manually detached. The kernels were sun-dried to reduce their water content. The separation of the thin cover from the kernel was carried out using a hammer to blow off the cover to obtain a maximum yield of oil. Using a mechanical mill, the kernels derived from the seeds were adequately ground. After grinding, the particle size of the samples was in the range of 2–5 mm. Figure 1a shows the MKSO samples used in this study.

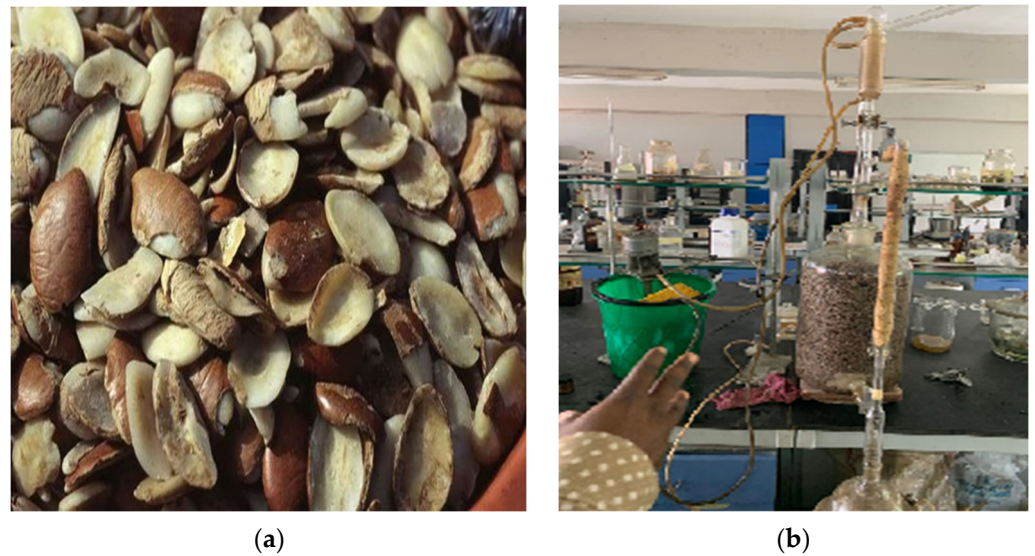


Figure 1. (a) Mango kernel seed samples; (b) Extraction process of MKSO.

2.2. Oil Extraction Process

The oil from the seeds can be extracted by employing some techniques, including conventional extraction, supercritical fluid extraction, solvent extraction, and mechanical means. In this study, solvent extraction was adopted. Solvent extraction is by far the most effective method of oil extraction because of the large amount of oil obtained from seeds. Solvent extraction fills the hole between supercritical fluid extraction, which is costly to develop and sustain, and mechanical extraction, which yields oil with high turbidity metal and moisture content. Hexane is commonly utilized as a solvent for the extraction of oil because of its lower thermal conductivity, which enables easy separation upon extraction, as well as its nonpolar nature, which makes it ideal for extracting nonpolar vegetable oils. According to the AOAC [19] approach, oil samples were obtained using a 5-liter, rounded volumetric flask; a Soxhlet system; and reagent-grade n-hexane with a boiler temperature of 40–60 °C. Figure 1b shows the extraction process of MKSO.

2.3. Characterization of Crude Oil Extracts

Raw MKSO extracts were characterized to identify phytochemistry (such as Fourier transform infrared analysis and gas chromatography), physio-chemical (specific gravity, crude oil pH, oil yield, viscosity, and oil color), and lubricity-related properties (flash point, fire point, cloud point, and pour point). These tests were conducted to determine effective specifications for the composition of cutting fluid. The determination of physicochemical, phytochemical, and thermal properties is presented in Table 1.

$$\text{Specific gravity} = \frac{\text{weight of oil}}{\text{weight of an equal volume of water}} \quad (1)$$

$$\% \text{ Oil yield} = \frac{\text{weight of extracted oil}}{\text{weight of powder sample}} \times 100 \quad (2)$$

$$\eta = U(\rho \times t) - V \frac{d}{t} \quad (3)$$

where ρ = density in g/mL, η = viscosity in centipoises (cP), t = time in seconds, U and V are constants.

Table 1. Determination of physicochemical, phytochemical, and thermal properties.

S/N	Parameter	Methodology
1	Fourier transform infrared analysis	This was determined by using a PerkinElmer FT-IR Spectrum in the 4000–400 cm^{-1} range. The precision was eight and two scans. Sample extracts were spread on KBR cells, inserted into the cell holder, and placed in the FT-IR spectrophotometer
2	Gas chromatography	This was obtained with a combined 7890A Agilent Technology GC system. During the process, oil was split into its chemical constituents. The column features of this machinery are as follows: HP5MS, 30 m \times 0.320 mm, 0.25 m width, helium carrier gas, and 2.5 mL/min flow rate. At a rate of 10 $^{\circ}\text{C}/\text{min}$, the temperature range was configured between 80 and 280 $^{\circ}\text{C}$. The splitless injector and detector were kept at 250 and 200 $^{\circ}\text{C}$, respectively.
3	Crude oil pH	A digital pH meter was used to determine the pH of raw mango oil.
4	Specific gravity	This was obtained based on ASTM D287 procedure and was further calculated using Equation (1) [20].
5	% Oil yield	The percentage oil yield was calculated using Equation (2).
6	Viscosity	This was determined using an Oswald kinematic viscometer in the temperature range of 40–80 $^{\circ}\text{C}$, and was further evaluated using Equation (3).
7	Oil color	The color of the oil was evaluated using a spectrophotometer and the Cc 13c -50 AOCS standard technique was adopted.
8	Pour point	This was examined with a Stanhope–Seta pour and cloud point KT16 8AP machinery based on ASTM D97 standards [21].
9	Cloud point	This was measured with Stanhope–Seta cloud/pour point KT16 8AP machinery and carried out according to ASTM D2500 [22].
10	Flashpoint	The flashpoint was measured by using an ASTM D92 conventional method [23].
11	Fire point	This was measured according to the ASTM D92 method with a Pensky–Martens setup.

ASTM—American Society for Testing and Materials; AOCS—American Oil Chemists Society.

2.4. Formulation of Cutting Fluids Emulsion

The vegetable oil was used to produce emulsion cutting fluid. Viscous washing soap (8–12 mL), sodium molybdate (1–2 mL), triziane (0.5–1.0 mL), and silicones (0.5–1.0 mL) were added as additives to pure MKSO using 2^4 factorial design to determine the best combinations. The additives, decontaminated water, and vegetable oil were combined to develop the MKSO emulsion. Emulsions with 20% oil-to-water volume samples were prepared to employ 16 assays derived from factorial design techniques [24,25]. As shown in Table 2, each experiment had a total concentration of 100 mL. The aim was to study the best composition for these formulations and the efficiency of the additives. At a room temperature of 25 $^{\circ}\text{C}$, this solution was stirred with a mechanical stirrer at 760 rpm for 10 min. The 16 experimental assays were characterized using pH and were compared with the equivalent of conventional MOCF emulsion.

Table 2. Volumes of cutting fluids for preliminary formulation.

Assay No	A (mL)	B (mL)	C (mL)	D (mL)	Vol. of Water (mL)
1	8	1	0.5	0.5	70
2	12	1	0.5	0.5	66
3	8	2	0.5	0.5	69
4	12	2	0.5	0.5	65
5	8	1	1.0	0.5	69.5
6	12	1	1.0	0.5	65.5
7	8	2	1.0	0.5	68.5
8	12	2	1.0	0.5	64.5
9	8	1	0.5	1.0	69.5
10	12	1	0.5	1.0	65.5
11	8	2	0.5	1.0	68.5
12	12	2	0.5	1.0	64.5
13	8	1	1.0	1.0	69
14	12	1	1.0	1.0	65
15	8	2	1.0	1.0	68
16	12	2	1.0	1.0	64

A—Emulsifier (viscous washing soap), B—anticorrosive agent (sodium molybdate), C—biocides (triziane), D—antifoam agent (silicones).

2.5. Evaluation of pH of Emulsion Cutting Fluids

The pH of a cutting fluid indicates its quality and stability. A drop in pH implies that the cutting fluid's performance has deteriorated. Excessively high or low pH values can be harmful to humans and cause hazardous waste issues. The pH test was performed using a digital pH meter shown in Figure 2. The responses of the pH values were subjected to statistical analysis using Minitab 16 application (Design of Experiment). The analysis software employs a second-degree polynomial, approximated by Equation (4), to predict the response, X , which includes all factors as well as the most accurate means for the factors to interact.

$$X = \varphi_0 + \sum \varphi_i Y_i + \sum \varphi_{ii} Y_i^2 + \sum \varphi_{ij} Y_i Y_j \quad (4)$$

where φ_0 is constant φ_i and φ_{ij} are coefficient of ij , x_i represents independent variables, and y_{ij} denotes the interrelation thereof [26]. The best values obtained were used to develop the final emulsion metal cutting fluids used for machining in this study.

**Figure 2.** pH testing of MKSO.

2.6. Machining Operations

Before machining operations, four pieces of workpiece materials with dimensions of 1500 mm in length and 80 mm in diameter were purchased from Ibadan, Nigeria. The workpiece was subsequently reduced in length to 320 mm while the diameter remained 80 mm. This was required to ensure a 1 to 4 ratio of turning operation initial diameter to length of the workpiece to guarantee the workpiece, chuck, and cutting force stiffness required [27]. Chemical analysis of the workpiece sample was carried out using an optical electron spectrometer. A tensile test was conducted on the workpiece with the aid of a computerized instron electromechanical universal tensile testing machine (see Figure 3). The machining was accomplished on an AJAX lathe, and the cutting tools were tungsten carbide insert tools with the model number CNMG12040408. Spindle speeds (355, 500, and 710 rpm), feed rates (0.1, 0.15, and 0.2 mm/rev), and depth of cuts (0.75, 1.0, and 1.25 mm) were all considered as factors and at varying levels (low, medium, and high). The influences of MKSO emulsion on cutting temperature, machine sound level, machine vibration, and surface roughness while turning AISI 1525 steel with a cemented carbide tool were evaluated in comparison to MOCF. The experimental plan was based on the Taguchi L_9 (3^3) orthogonal array, shown in Table 3.



Figure 3. Tensile testing of AISI 1525 steel.

Table 3. Standard Taguchi L_9 (3^3) orthogonal array.

Trial No.	Cutting Parameter		
	Spindle Speed (rev/min)	Feed Rate (mm/rev)	Depth of Cut (mm)
1	355	0.1	0.75
2	355	0.15	1.00
3	355	0.20	1.25
4	500	0.1	1.00
5	500	0.15	1.25
6	500	0.20	0.75
7	710	0.1	1.25
8	710	0.15	0.75
9	710	0.20	1.00

2.7. Determination of Surface Roughness

The surface roughness of the workpiece material was measured using an SRT6200 handheld surface-roughness analyzer. For every sample, three tests were conducted arbitrarily along the workpiece length, and the estimated value was used for analysis.

2.7.1. Determination of Cutting Temperature

Cutting temperature was recorded with a PeakTech Infrared thermometer and an emissivity value of 0.12 specified by Calex Electronics Limited for AISI 1525 steel. The degree of hotness at the chip–tool interface was measured by pointing the thermometer’s probe at the interface during machining. The infrared temperature sensor was manually held 5 cm away from the chip–tool interface. For each sample, three samples were recorded, and the average reading was calculated.

2.7.2. Determination of Machine Vibration

Vibrations are unavoidable during the machining operation. Vibration from the machine for different cutting conditions was determined using a VB8206SD Lutron vibration meter. The vibration meter probe was placed beside the machine’s headstock, very close to the spindle. The meter gives its reading in terms of displacement, velocity, and acceleration, but the reading for this study was taken in terms of acceleration (m/s^2). It can record the minimum and maximum spindle vibration over time.

2.7.3. Determination of Machine Sound Level

Noise from the machine for different cutting conditions was determined by a sound level meter (Testo815), which uses a sound recording and analysis software application called Cool Edit. The software application was opened, and the noise recording interface was configured to a sample rate of 96,000, stereo channels, and a 32-bit (float) resolution. The laptop was placed about 1.2 m away from the machine.

3. Results and Discussion

3.1. Phytochemical Characterization of MKSO Extracts

The FT-IR spectra of MKSO show the presence of a broad vibrational band between $3370\text{--}2400\text{ cm}^{-1}$ indicative of the -OH stretching vibrational band of carboxylic acid. The bands at 2923 cm^{-1} and 2852 cm^{-1} are assigned to the -C-H stretching vibrational bands of -CH_2 and -CH_3 respectively, while the bands at 1702 cm^{-1} , 1461 cm^{-1} , 1290 cm^{-1} , and 935 cm^{-1} are assigned to the carbonyl (-C=O) stretching band, -C-H bending of -CH_2 , -C-O stretching, and -OH bending vibrational bands [10]. Figure 4 depicts a typical FT-IR spectrum of MKSO.

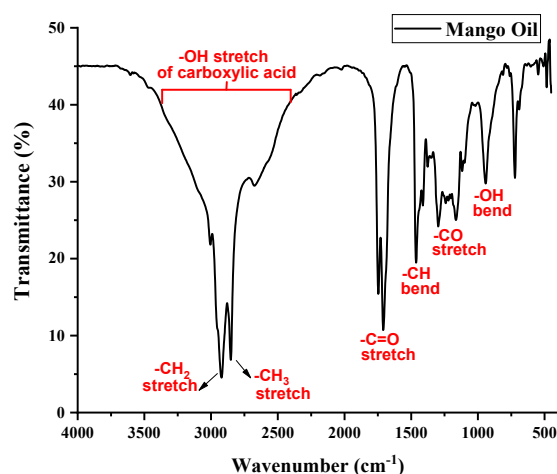


Figure 4. Fourier transforms infrared for crude MKSO.

Mango extracts were found to be abundant in four compounds: cis-vaccenic acid, hexadecanoic acid, 3-pentadactyl phenol, and squalene as depicted in Table 4. Fatty acids, phenol compounds, and unsaturated hydrocarbons constituted the isolated chemicals. The oil extracted is a bio-based combination with a synergistically absorbing ability, which could be a more substantive replacement for mineral-based lubricants with environmentally destructive antecedents. Compound 1 was discovered to be cis-vaccenic acid ($C_{18}H_{34}O_2$), with an $M+$ of 282 and a baseline peak at M/Z 55. This is due to the fragmentation of an alkyl (butyl) ion. The chemical has a composition of 0.59 percent and is found in trace concentrations of MKSO. Due to the McLafferty reaction, Compound 2 was discovered to be hexadecanoic acid $M+$ 256 with a characteristic base peak at M/Z 60 [28]. The compound is 38.76% by composition in the MKSO sample. Hexadecanoic acid is the second-most abundant compound in the MKSO sample. Hexadecanoic acid has a wide range of applications, including cosmetics and soaps. Although hexadecanoic acid has not yet been reported in the use of cutting fluids, it can be given an attempt due to its use in personal care items, i.e., it is humanly acceptable. The MKSO is made up of bio-based compounds with a synergistic penetrating power that could be a superior long-term replacement for mineral-based lubricants that are environmentally harmful. 3-Pentadactyl phenol ($C_{21}H_{36}O$), $M+$ 304, with a base peak of 108, was discovered in Compound 3. This is a fragment of benzyl alcohol polar ion. According to the chemistry of the isolated MKSO, the substance is 4.18%. Due to the polarization of an alkyl residue, Compound 4 was determined to be squalene ($C_{30}H_{50}$), $M+$ 410, and a base peak of 69 (pentyl). The substance is a crucial step in the production of triterpenoids. Squalene accounts for 2.51% of the extracted MKSO content. Squalene is utilized in cosmetology and, more recently, in vaccinations as an immunologic additive. Squalene is anticipated to offer some resistance to certain forms of cancer [29,30]. The mass spectra of MKSO compounds are shown in Figure 5.

Table 4. Gas chromatography analysis of phytocompounds isolated from MKSO.

Oil	Chromatography Peak	Compound Nomenclature	Molecular Formula	Molecular Weight	Retention Time (min)	Percentage Content
Mango kernel seed oil	1	cis-vaccenic acid	$C_{18}H_{34}O_2$	282	19.822	55.28
	2	n-hexadecanoic acid	$C_{16}H_{32}O_2$	256	17.627	38.76
	3	3-pentadecyl phenol	$C_{21}H_{36}O$	304	26.488	4.18
	4	Squalene	$C_{30}H_{50}$	410	29.898	2.51

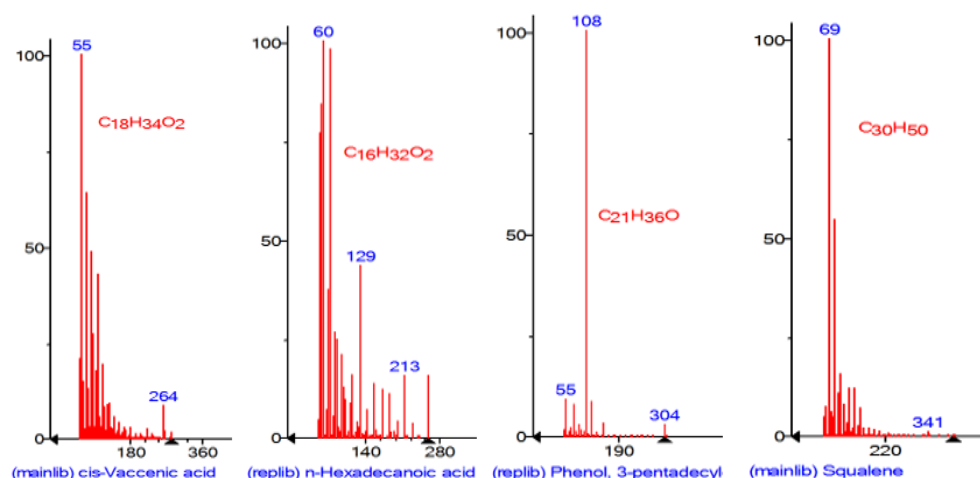


Figure 5. Mass spectra of isolated phytocompounds.

3.2. Physicochemical and Thermal Properties Characterization of MKSO Extracts

The results of the physicochemical and thermal properties of MKSO extract are shown in Table 5. The MKSO was brownish yellow. The oil content in MKSO was observed to be 12% by the weight of their seeds. The oil content was in line with what was obtained by Karunanithi et al. [31]. MKSO has a higher oil content than some vegetable oils, such as soybean oil, which has been considered by several studies as a bio-based cutting fluid [5,9,12,32,33]. Soybean oil has an oil content ranging from 11 to 25%. The MKSO sample had a specific gravity of 0.833, which is within the range of specific gravities recorded for similar vegetable oils of a few tropical plants. According to Aremu et al. [34], the specific gravity of various seed oils varies between 0.830 and 1.710. Vegetable oils in the aforementioned specific gravity range are less dense than water and hence advantageous in lubricant manufacturing because this property allows the oils to flow and spread easily over the workpiece [35]. MKSO has a viscosity of 16.8. The viscosity of MKSO was within the range of values found in the literature, which ranged from 0.43 to 302.39. Melon, castor, and almond-seed oils have viscosities of 5.89, 9.42, and 302.39. The higher the viscosity of an oil, the better its use as a lubricant [36]. Oils with a low viscosity indicate that they are light and thus non-polar [34]. The MKSO sample had a pH of 6.5, thereby denoting that it is acidic. A workpiece may corrode during machining processes if the pH is less than 7.0. The presence of various contaminants and other constituents of the crude oil composition, such as the solvent employed in the extraction, could account for the drop in the pH of the MKSO.

Table 5. Physicochemical and thermal properties of MKSO.

Parameter	Result
pH	6.5
Specific gravity	0.833
% Oil yield	12.5
Viscosity	16.8 cP
Oil color	Brownish Yellow
Pour point	36
Cloud point	39
Flashpoint	158
Fire point	167

Tables 6 and 7 show the chemical and mechanical properties of the workpiece, respectively. The results confirmed the type of steel (workpiece) employed in the study. The steel is made up of 16 elements, such as carbon, silicon, manganese, sulfur, phosphorus, chromium, nickel, copper, aluminum, boron, iron, vanadium, tungsten, and molybdenum. Iron has the highest proportion among all the elements. According to AISI/SAE specifications and based on the chemical properties presented, the steel's number is AISI 1525 steel. The machined materials are presented in Figure 6.

Table 6. Chemical properties of AISI 1525 steel.

Element	% Composition
C	0.2505
Si	0.2215
Mn	1.2340
S	0.0235
P	0.0135
Cr	0.1135
Ni	0.1155
Cu	0.0480
Al	0.0120
Ti	0.0395
Fe	97.9285

Table 7. Mechanical properties of AISI 1525 steel.

Properties	Result
Tensile Strength	604.74 MPa
Yield Strength	7599.34 MPa
Elastic Modulus	35106.19MPa
Energy at Maximum Tensile Stress	31.24909 J
Energy at Break	47.35634 J

**Figure 6.** Machined AISI 1525 steel.

3.3. Experimental Results for AISI 1525 Steel Machining with Emulsion Cutting Fluids

The results of the experiment carried out using the formulated mango kernel seed oil and mineral oil are shown in Tables 8 and 9, respectively. It can be observed that surface roughness, cutting temperature, sound level, and machine vibration of emulsion cutting fluids fell within the ranges of 2.53–9.63 μm , 36.7–82.7 $^{\circ}\text{C}$, 96.5–106.3 dB, and 14.5–67.8 ms^{-2} ; and 2.545–8.83 μm , 46.8–111.8 $^{\circ}\text{C}$, 85.7–111.1 dB, and 7.91–42.9 for mango-kernel-seed-oil- and mineral-oil-based cutting fluids, respectively. In general, the surface roughness, cutting temperature, machine sound level, and machine vibrations were 6.984 ± 2.83 and 6.67 ± 2.27 μm , 55.91 ± 13.13 and 81.48 ± 26.49 $^{\circ}\text{C}$, 103.99 ± 3.151 and 97.18 ± 11.63 dB, 44.60 ± 17.83 and 23.94 ± 10.68 m/s^2 for MKSO and MOCF, respectively. Good machining is obtained with reduced surface roughness, cutting temperature, machine vibration, and noise levels for the environment. From the aforementioned results of process parameters, MOCF performed exceedingly better than MKSO.

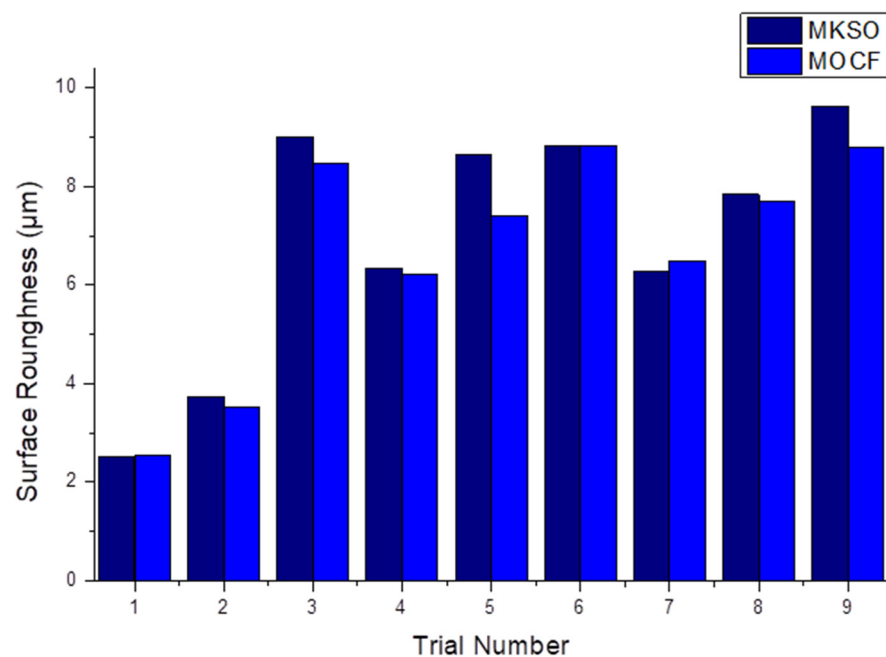
Table 8. Experimental results of MKSO cutting fluids.

Spindle Speed (rev/min)	Feed Rate (mm/rev)	Depth of Cut (mm)	Surface Roughness (μm)	Cutting Temp. ($^{\circ}\text{C}$)	Sound Level (dB)	Machine Vibration (m/s^2)
355	0.1	0.75	2.53	36.7	96.5	14.5
355	0.15	1	3.73	55.8	102.5	25.42
355	0.2	1.25	9.01	50.2	106.1	51.7
500	0.1	1	6.35	57.2	106.2	43.9
500	0.15	1.25	8.65	51.8	106.3	31.7
500	0.2	0.75	8.83	68.9	103.1	45.2
710	0.1	1.25	6.29	82.7	103.9	61.4
710	0.15	0.75	7.84	49.4	105.4	59.8
710	0.2	1	9.63	50.5	105.9	67.8

Table 9. Experimental results of MOCFs.

Spindle Speed (rev/min)	Feed Rate (mm/rev)	Depth of Cut (mm)	Surface Roughness (μm)	Cutting Temp. ($^{\circ}\text{C}$)	Sound Level (dB)	Machine Vibration (m/s^2)
355	0.1	0.75	2.545	46.8	85.7	27.03
355	0.15	1	3.521	57.2	85.9	7.91
355	0.2	1.25	8.47	59.8	86	28.7
500	0.1	1	6.22	76.6	85.7	15.5
500	0.15	1.25	7.41	60.2	95.5	42.9
500	0.2	0.75	8.83	105.5	108.8	21.4
710	0.1	1.25	6.5	106.2	106.9	29.2
710	0.15	0.75	7.7	109.2	111.1	12.9
710	0.2	1	8.8	111.8	109	29.95

Figures 7–10 show the effect of input parameters (spindle speed, depth of cut, and feed rate) on surface roughness, cutting temperature, vibration rate, and machine sound level. Figure 7 depicts the surface roughness chart for the two emulsion cutting fluids throughout nine trials. In general, the surface roughness of the MOCF was the best between the emulsified metal cutting fluids over the nine experiments. In 75% of the experiments, MOCF had the lowest surface roughness values. The lowest surface roughness was obtained for MKSO at a low spindle speed, while the maximum surface roughness was obtained for the same oil at high speed. The surface roughness of the two emulsion cutting fluids increased as the spindle speed increased from low to moderate rates: however, as the spindle speed rose from a moderate to a high speed, the surface roughness of MOCF gradually diminished while that of MKSO marginally increased. The surface roughness of the two cutting fluids significantly increased as the feed rate increased from low to moderate speeds. Moreover, as the feed rate increased from moderate to high, the surface roughness of all emulsion cutting fluids sharply increased. The surface roughness of MOCF increased as the depth of cut decreased from low to moderate, whereas the surface roughness of MOCF sharply increased as the depth of cut extended from moderate to high. Meanwhile, the surface roughness of MKSO gradually increased from low to high depth of cut, with a faster increase from moderate to high depth of cut.

**Figure 7.** Effect of emulsion cutting fluids on surface roughness of AISI 1525 steel.

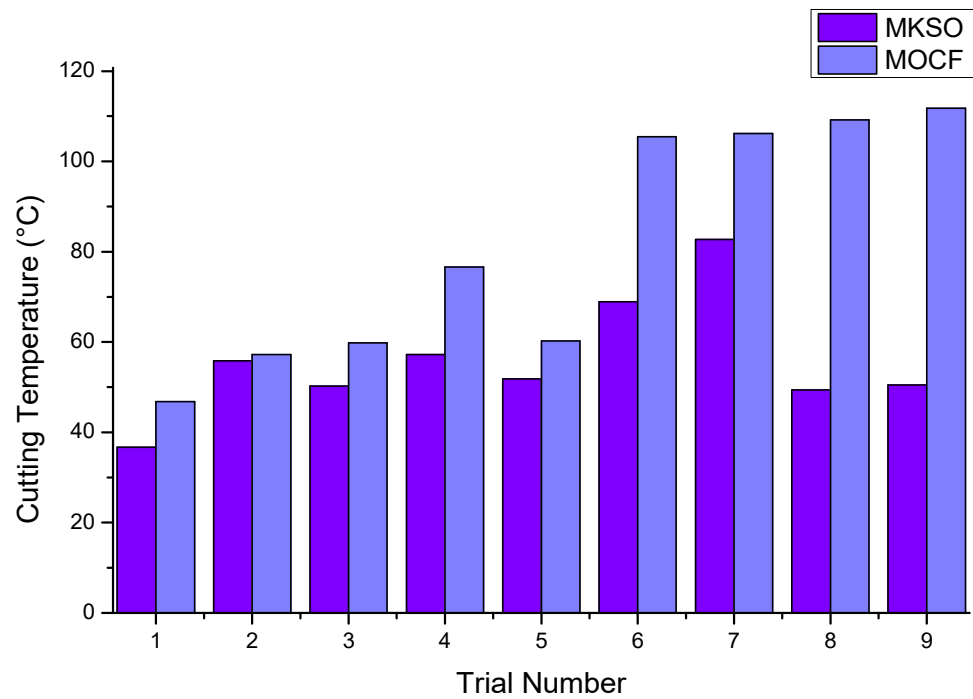


Figure 8. Effect of emulsion cutting fluids on cutting temperature of AISI 1525 steel.

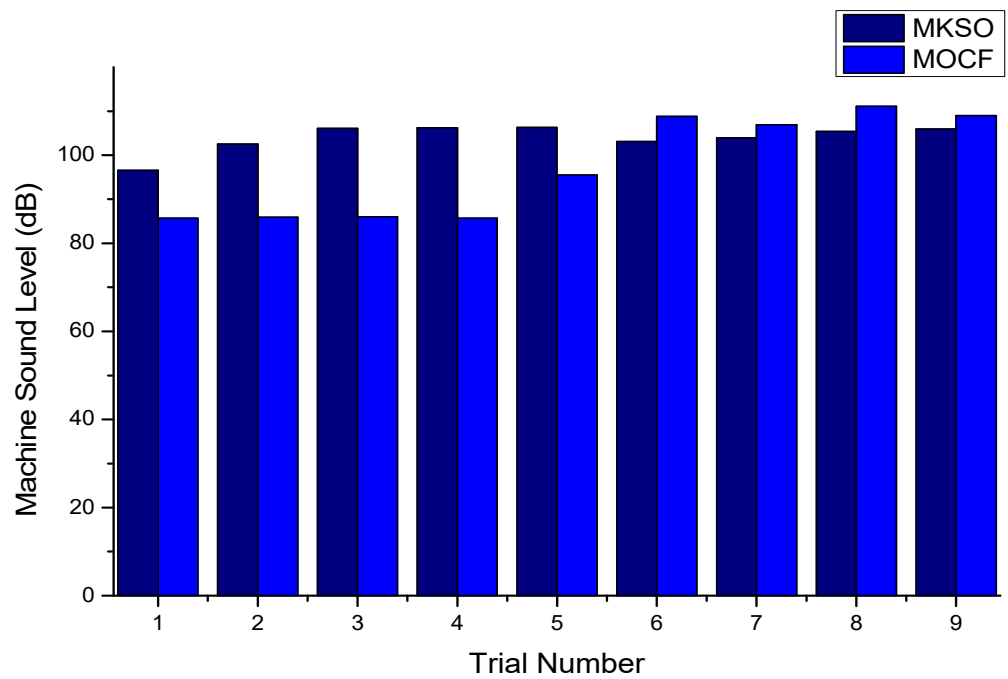


Figure 9. Effect of emulsion cutting fluids on machine sound level of AISI 1525 steel.

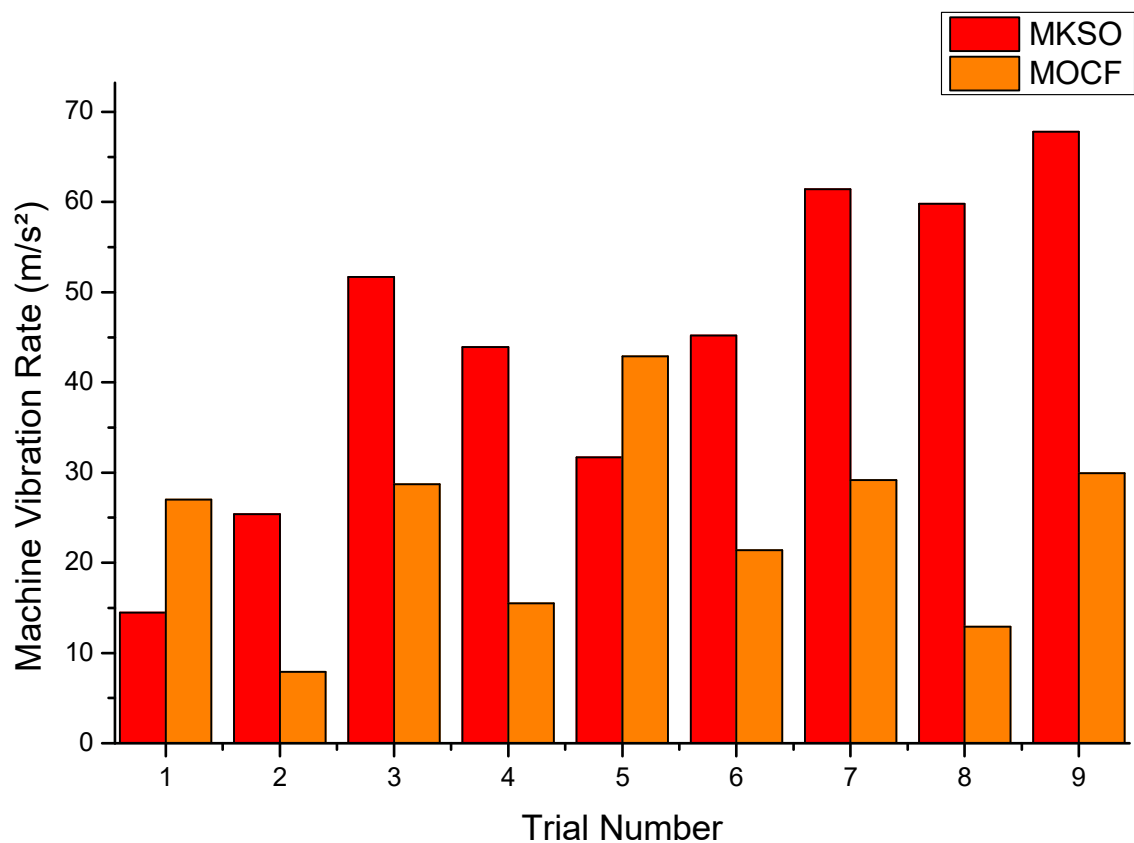


Figure 10. Effect of emulsion cutting fluids on machine vibration rate of AISI 1525 steel.

The cutting temperature increased as the depth of cut increased from low to moderate depth of cut for MKSO, while it continuously increased from moderate to high for MKSO. On the other hand, the cutting temperature of MOCF decreased gently and continuously from low to high depth of cut. Figure 8 shows the cutting temperature findings for the two oils investigated during the nine trials. MKSO had the lowest cutting temperature in any of the trials performed during the testing. Based on the effect of cutting parameters on cutting temperature, it was apparent that for MOCF and MKSO, the cutting temperature increased as the speed increased from low to moderate. Nevertheless, as spindle speeds increased, the cutting temperature of MKSO lowered significantly, while that of MOCF rose. Using the two emulsion conditions, the variation of feed rate on cutting temperature showed that the temperature was maximum at a high feed rate with MOCF. The variation between the depth of cut and cutting temperature under the two emulsion conditions was observed.

In the course of the nine trials, MOCF had the lowest machine sound level in five machining trials (see Figure 9). The effects of spindle speed on machine sound level, at various spindle speeds, for the two-emulsion oil under study showed that MKSO had a gentle increase in machine sound level from 101 dB to 104 dB between 355 rev/min and 500 rev/min; while a slight, insignificant decrease was observed between 500 rev/min and 710 rev/min. MOCF increased throughout the three spindle-speed points. Notable is that the two emulsion fluids obtained their minimum sound levels at spindle speed 355 rev/min. MKSO reached its maximum sound level at 500 rev/min, while MOCF reached its maximum sound level at 710 rev/min. MOCF also showed a drastic decrease between depths of cut 0.75 and 1.0 mm from 102dB to 94dB, while there was a gentle increase from 94–96 dB between depths of cut 1.00 and 1.25 mm. It produced the least sound level at 1.0 mm. The mango emulsion showed a different pattern from the rest by increasing from 101.5dB to 104.5 dB to 105 dB between depths of cut 0.75, 1.0, and 1.25 mm. It produced the lowest sound level at 0.75 mm.

Figure 10 shows that MKSO exhibited a slight increase in machine vibration rate from 30 m/s² to 40 m/s² between 355 rev/min and 500 rev/min, while a much more significant increase was observed between 500 and 710 rev/min from a vibration rate of 40 m/s² to 60 m/s². The vibration rate observed on the machine with MKSO rose and dropped down alternatively at the three spindle-speed points, starting at 22 m/s² to 25 m/s² and back to 20 m/s², respectively. MKSO reached its minimum machine vibration rate at spindle speed 355 rev/min, while MOCF reached its minimum machine vibration rate at 710 rev/min. MKSO showed an alternating slight decrease and rapid increase between 0.1 and 0.2 mm/rev; the lowest vibration rate was observed at a feed rate of 0.15mm/rev. MOCF produced an alternating decrease and increase between 0.1 and 0.2 mm/rev; the lowest vibration rate was observed at a feed rate of 0.15 mm/rev. MOCF also showed a gentle decrease in machine vibration rate between depths of cut 0.75 and 1.0 mm from 20 m/s² to 17 m/s², with a rapid increase from 17 m/s² to 35 m/s² between depths of cut 1.00 and 1.25 mm. It produced the lowest vibration rate at 1.0 mm. MKSO showed an insignificant increase in machine vibration rate from 40 m/s² to about 47 m/s² between depths of cut 0.75 and 1.25 mm. The lowest vibration rate was produced at 0.75 mm.

3.4. Grey Relational Analysis

The method for obtaining the grey relational grade is detailed in Table 10.

$$y^*_j(n) = \frac{\max y_j(n) - y_j(n)}{\max y_j(n) - \min y_j(n)} \tag{5}$$

$$\varphi_j(n) = \frac{\chi_{\min} + \varphi\chi_{\max}}{\chi_{oj}(n) + \varphi\chi_{\max}} \tag{6}$$

$$\lambda_j = \frac{1}{m} \sum_{k=1}^m \varphi_j(k) \tag{7}$$

Table 10. Steps to a successful Grey relational analysis.

Step	Action
1.	To avoid using different units and to reduce variability, the data must first be standardized. It is generally required since the variation of one datum differs from other data. The array is made between 0 and 1 by calculating an appropriate value from the original value [37]. It is a way of converting original data to equivalent data in general. If the response is to be reduced, Equation (5) is used to normalize it into an appropriate range using smaller-is-better characteristics. From the relation, $j = 1, \dots, u; n = 1, \dots, q; n$ is the number of responses, while p is the number of experimental results. $y_j(n)$ represents the real series, $\max y_j(n)$ represents the highest value of $y_j(n)$, $\min y_j(n)$ represents the lowest value of $y_j(n)$, $y^*_j(n)$ represents the series after the result pre-processing, and y is the desired value [37].
2.	Equation (6) is used to compute the Grey relational coefficient, $\varphi_j(n)$, from the normalized data. The χ_{oj} in the equation is divergence series of the reference series and the comparability series and $\chi_{oj} = \ y_o(n) - y_j(n)\ $. $y_o(n)$ refers to the reference series and $y_j(n)$ is known as comparability series. χ_{\max} and χ_{\min} are the maximum and minimum values of the absolute differences χ_{oj} of all series being compared. φ is a distinguishing coefficient and ranges between 0 and 1. Most times, the value of φ is 0.5.
3.	The Grey relational grade (GRG) is calculated with Equation (7). From the equation, γ_i is the necessary GRG for j th trial and $m = \text{no. of response characteristics}$. The GRG denotes the level of correlation between the comparability series and the reference series and is the all-encompassing representation of all qualitative attributes [37]. Therefore, using GRA and the Taguchi technique, the multiple response optimization models is reduced to just one response optimization model.
4.	Then, using a higher GRG, an appropriate level of process variables is obtained, indicating the greater quality of the product. To determine this, the mean grade values for individual level of process parameters are to be obtained, which can be shown as a mean response chart. From the mean response chart, the greater value of mean grade values is selected as the best parametric combination for multiple responses.
5.	After determining the best combination, the analysis of variance (ANOVA) is used to find the major parameters affecting the multiple responses at a 95% confidence level, providing useful information on the experimental results. Since the Taguchi technique cannot assess the influence of each parameter on multiple responses, the ANOVA will be useful in determining the percentage of contribution to evaluate the influence. The ANOVA approach divides the entire variability of the output (sum of squared deviations around the weighted score) into contributions from each parameter and error [37].

3.5. Application of Grey Relation Analysis to Obtain Multiple Responses Parametric Optimizations

Tables 11 and 12 show the experimental results obtained from the laboratory during the cylindrical turning of AISI 1525 steel alloy. In the process of standardizing the experimental results, the maximum and minimum values for each process parameter were obtained. Equation (5) was used to normalize the experimental results for cutting temperature, surface roughness, machine sound level, and machine vibration. The results are provided in Tables 13 and 14 as Grey relational generations for both mango kernel seed oil cutting fluid and mineral-oil-based cutting fluid. Tables 15 and 16 present the deviation sequence for MKSO and MOCF, respectively. The deviation sequence is a requirement or prerequisite in determining the Grey relational coefficients.

Table 11. Experimental results of MKSO cutting fluids.

Spindle Speed (rev/min)	Feed Rate (mm/rev)	Depth of Cut (mm)	Surface Roughness (μm)	Cutting Temp. ($^{\circ}\text{C}$)	Sound Level (dB)	Machine Vibration (m/s^2)
355	0.1	0.75	2.53	36.7	96.5	14.5
355	0.15	1	3.73	55.8	102.5	25.42
355	0.2	1.25	9.01	50.2	106.1	51.7
500	0.1	1	6.35	57.2	106.2	43.9
500	0.15	1.25	8.65	51.8	106.3	31.7
500	0.2	0.75	8.83	68.9	103.1	45.2
710	0.1	1.25	6.29	82.7	103.9	61.4
710	0.15	0.75	7.84	49.4	105.4	59.8
710	0.2	1	9.63	50.5	105.9	67.8
		Min	2.53	36.7	96.5	14.5
		Max	9.63	82.7	106.3	67.8

Table 12. Experimental results of MOCFs.

Spindle Speed (rev/min)	Feed Rate (mm/rev)	Depth of Cut (mm)	Surface Roughness (μm)	Cutting Temp. ($^{\circ}\text{C}$)	Sound Level (dB)	Machine Vibration (m/s^2)
355	0.1	0.75	2.545	46.8	85.7	27.03
355	0.15	1	3.521	57.2	85.9	7.91
355	0.2	1.25	8.47	59.8	86	28.7
500	0.1	1	6.22	76.6	85.7	15.5
500	0.15	1.25	7.41	60.2	95.5	42.9
500	0.2	0.75	8.83	105.5	108.8	21.4
710	0.1	1.25	6.5	106.2	106.9	29.2
710	0.15	0.75	7.7	109.2	111.1	12.9
710	0.2	1	8.8	111.8	109	29.95
		Min	2.545	46.8	85.7	7.91
		Max	8.83	111.8	111.1	42.9

Table 13. Grey relational generation values for MKSO cutting fluids.

Normalization			
Surface Roughness (μm)	Cutting Temp. ($^{\circ}\text{C}$)	Sound Level (dB)	Machine Vibration (m/s^2)
1.000	1.000	1.000	1.000
0.831	0.585	0.388	0.795
0.087	0.707	0.020	0.302
0.462	0.554	0.010	0.448
0.138	0.672	0.000	0.677
0.113	0.300	0.327	0.424
0.470	0.000	0.245	0.120
0.252	0.724	0.092	0.150
0.000	0.700	0.041	0.000

Table 14. Grey relational generation values for MOCFs.

Normalization			
Surface Roughness (μm)	Cutting Temp. ($^{\circ}\text{C}$)	Sound Level (dB)	Machine Vibration (m/s^2)
1.000	1.000	1.000	0.454
0.845	0.840	0.992	1.000
0.057	0.800	0.988	0.406
0.415	0.542	1.000	0.783
0.226	0.794	0.614	0.000
0.000	0.097	0.091	0.614
0.371	0.086	0.165	0.392
0.180	0.040	0.000	0.857
0.005	0.000	0.083	0.370

Table 15. Deviation sequence for MKSO.

Surface Roughness (μm)	Cutting Temp. ($^{\circ}\text{C}$)	Sound Level (dB)	Machine Vibration (m/s^2)
0.000	0.000	0.000	0.000
0.169	0.415	0.612	0.205
0.913	0.293	0.980	0.698
0.538	0.446	0.990	0.552
0.862	0.328	1.000	0.323
0.887	0.700	0.673	0.576
0.530	1.000	0.755	0.880
0.748	0.276	0.908	0.850
1.000	0.300	0.959	1.000

Table 16. Deviation sequence for MOCF.

Surface Roughness (μm)	Cutting Temp. ($^{\circ}\text{C}$)	Sound Level (dB)	Machine Vibration (m/s^2)
0.000	0.000	0.000	0.546
0.155	0.160	0.008	0.000
0.943	0.200	0.012	0.594
0.585	0.458	0.000	0.217
0.774	0.206	0.386	1.000
1.000	0.903	0.909	0.386
0.629	0.914	0.835	0.608
0.820	0.960	1.000	0.143
0.995	1.000	0.917	0.630

Equation (6) was used to obtain Grey relational coefficients from the normalized data set. As both quality attributes were given equal weighting, the value of the distinguishing coefficient was set to 0.5. Tables 15 and 16 display the results. The GRG was then calculated from the Grey relational coefficients using Equation (7). Tables 17 and 18 show the results of the GRG. As it is transformed to a single grade, the result is used to optimize the multi-responses.

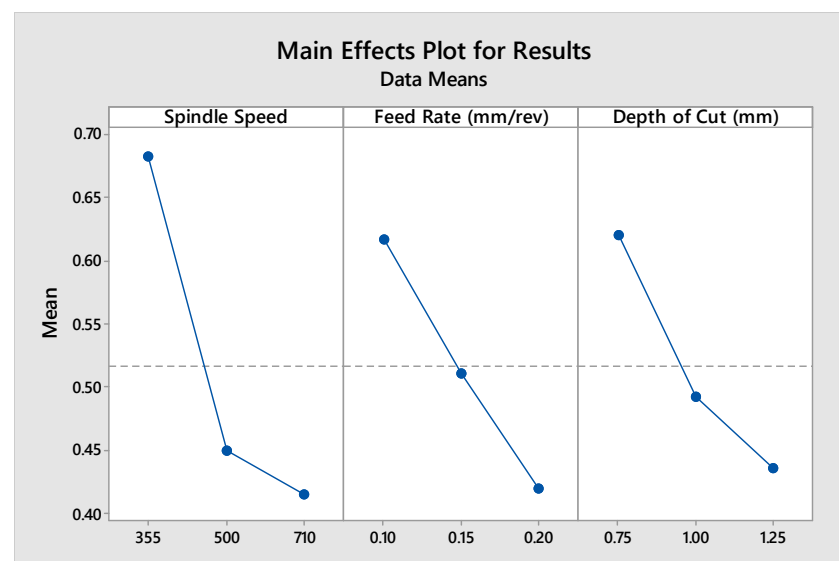
Table 17. Grey relational coefficient and grade relational grade for MKSO.

Surface Roughness (μm)	Cutting Temp. ($^{\circ}\text{C}$)	Sound Level (dB)	Machine Vibration (m/s^2)	Grade	Rank
1.000	1.000	1.000	1.000	1.000	1
0.747	0.546	0.450	0.709	0.613	2
0.354	0.630	0.338	0.417	0.435	6
0.482	0.529	0.336	0.475	0.455	4
0.367	0.604	0.333	0.608	0.478	3
0.360	0.417	0.426	0.465	0.417	7
0.486	0.333	0.398	0.362	0.395	9
0.401	0.644	0.355	0.370	0.443	5
0.333	0.625	0.343	0.333	0.409	8

Table 18. Grey relational coefficient and grade relational grade for MOCF.

Surface Roughness (μm)	Cutting Temp. ($^{\circ}\text{C}$)	Sound Level (dB)	Machine Vibration (m/s^2)	Grade	Rank
1.000	1.000	1.000	0.478	0.869	2
0.763	0.758	0.984	1.000	0.876	1
0.347	0.714	0.977	0.457	0.624	4
0.461	0.522	1.000	0.697	0.670	3
0.392	0.708	0.564	0.333	0.500	5
0.333	0.356	0.355	0.565	0.402	8
0.443	0.354	0.375	0.451	0.406	7
0.379	0.342	0.333	0.778	0.458	6
0.334	0.333	0.353	0.443	0.366	9

The effects of each cutting parameter at various levels are plotted and shown in Figures 11 and 12 for MKSO and MOCF, respectively. The mean GRG is shown in Tables 19 and 20 using the GRG values. The best parametric combination is determined by the highest mean GRG values in Tables 19 and 20 for MKSO and MOCF. The GRG with a greater value indicates a stronger correlation to the reference sequence and higher quality. Hence, for multi-responses, the best parameters for MKSO cutting fluid are SS1-FR1-DOC1—in other words, spindle speed of 0.683 rev/min, feed of 0.617 mm/rev, and depth of cut of 0.620 mm, respectively. The greater results of mean GRG give the minimum values of machine vibrations, surface roughness, machine sound level, and cutting temperature. The difference of highest (maximum) and lowest (minimum) values of mean GRG for turning parameters was 0.267 rev/min for spindle speed, 0.197 mm/rev for feed rate, and 0.184 mm for depth of cut, respectively (see Table 19). In turning operations with MKSO cutting fluids, this finding suggests that spindle speed has the greatest influence on multi-responses when contrasted with feed rate and depth of cut. The sequence of the significance of process parameters on multi-responses are spindle speed > feed rate > depth of cut. Table 20 illustrates the multi-responses for MOCF, with the best parameters being SS1-FR1-DOC2, or 0.7898 rev/min spindle speed, 0.6483 mm/rev feed, and 0.6373 mm depth of cut, respectively. For turning parameters, the difference between the greatest and lowest values of mean GRG was 0.3800 rev/min spindle speed, 0.1844 mm/rev feed rate, and 0.1278 mm depth of cut, respectively. This research reveals that, when compared to feed rate and depth of cut, spindle speed has the highest influence on multi-responses in turning operations with MOCFs. Spindle speed > feed rate > depth of cut is the order of effectiveness of process parameters on multi-responses.

**Figure 11.** Main effects plot for GRG (MKSO cutting fluid).

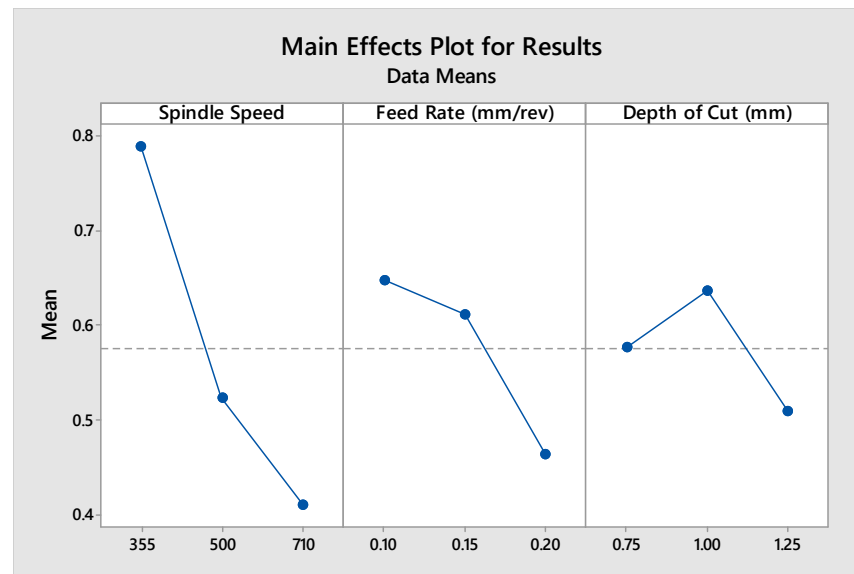


Figure 12. Main effects plot for GRG (MOCF).

Table 19. Main effects on mean GRG for MKSO.

Parameter	Level 1	Level 2	Level 3	Max-Min	Rank
Spindle Speed	0.683	0.450	0.415	0.267	1
Feed Rate	0.617	0.511	0.420	0.197	2
Depth of Cut	0.620	0.492	0.436	0.184	3

Total Mean Value of GRA: 0.5160.

Table 20. Main effects on mean GRG for MOCF.

Parameter	Level 1	Level 2	Level 3	Max-Min	Rank
Spindle Speed	0.7898	0.5239	0.4098	0.3800	1
Feed Rate	0.6483	0.6113	0.4639	0.1844	2
Depth of Cut	0.5766	0.6373	0.5096	0.1278	3

Total Mean Value of GRA: 0.5745.

Total Mean Value of GRA: 0.5160.

Furthermore, an analysis-of-variance table was prepared using the GRG values presented in Tables 21 and 22 for MKSO cutting fluid and MOCF, respectively. These ANOVA tables give the percentage contribution of process parameters on multi-responses. From the ANOVA table for MKSO cutting fluid, the contribution of each input parameter is given as follows: spindle speed (42.7036%), feed rate (19.5761%), and depth of cut (17.9487%). It shows that spindle speed has a significant influence on the multi-responses during the turning process of AISI 1525 steel. The influence of depth of cut and feed rate on multi-responses is less significant. On the other hand, the ANOVA analysis for MOCF, as shown in Table 22, shows the contribution of the cutting parameters as spindle speed (73.4513%), feed rate (18.3924%), and depth of cut (7.8897%). It also shows that spindle speed has the greatest contribution on MOCF multi-responses, followed by feed rate. The contribution of the depth of cut on the multi-responses is less significant. The confidence level specified for this analysis is 95%. It is revealed that spindle speed is the significant cutting parameter affecting multi-responses in the two cutting fluids being investigated [38,39]. Feed rate and depth of cut do not show many contributions to the responses of MKSO cutting fluid and MOCF.

Table 21. Results of ANOVA on GRG for MKSO cutting fluid.

Source	DF	Adj SS	Adj MS	F-Value	% Contribution
Spindle Speed (rev/min)	2	0.12674	0.06337	2.16	42.7036
Feed Rate (mm/rev)	2	0.05810	0.02905	0.99	19.5761
Depth of Cut (mm)	2	0.05327	0.02664	0.91	17.9487
Error	2	0.05868	0.02934		19.7716
Total	8	0.29679			100

Table 22. Results of ANOVA on GRG for MOCF.

Source	DF	Adj SS	Adj MS	F-Value	% Contribution
Spindle Speed (rev/min)	2	0.228100	0.114050	275.31	73.4513
Feed Rate (mm/rev)	2	0.057117	0.028559	68.94	18.3924
Depth of Cut (mm)	2	0.024501	0.012250	29.57	7.8897
Error	2	0.000829	0.000414		0.2669
Total	8	0.310546			100

3.6. Mathematical Model

At a 95 percent confidence level, a multiple regression model was created for two of the four parameters, such as surface roughness and cutting temperature, using the parameters: spindle speed (v), feed rate (f), and depth of cut (d). The model's adequacy was determined by calculating the value of its determination coefficients R^2 [37]. The larger the R^2 value, i.e., as it approaches 1, the greater the importance of the model. First- and second-order mathematical models for surface roughness and cutting temperature are described in Equations (8)–(15), together with their R^2 values for MKSO and MOCF, based on the experimental data. Surface roughness and cutting temperature are the parameters considered for the modeling because of their importance as major parameters of machining. Tables 23–30 show the summary of first- and second-order models.

Table 23. Model summary for surface roughness.

S	R^2	R^2 (adj)	R^2 (pred)
1.40745	79.92%	67.88%	48.48%

Table 24. Model summary for cutting temperature.

S	R^2	R^2 (adj)	R^2 (pred)
14.0329	28.56%	0.00%	0.00%

Table 25. Model summary for surface roughness.

S	R^2	R^2 (adj)	R^2 (pred)
1.35966	77.57%	64.12%	41.08%

Table 26. Model summary for cutting temperature.

S	R^2	R^2 (adj)	R^2 (pred)
11.0372	89.15%	82.64%	59.03%

Table 27. Model summary for surface roughness.

S	R ²	R ² (adj)	R ² (pred)
2.1124	92.63%	66.14%	62.65%

Table 28. Model summary for cutting temperature.

S	R ²	R ² (adj)	R ² (pred)
114.4545	94.03%	57.29%	51.71%

Table 29. Model summary for surface roughness.

S	R ²	R ² (adj)	R ² (pred)
3.2422	99.21%	36.49%	38.37%

Table 30. Model summary for cutting temperature.

S	R ²	R ² (adj)	R ² (pred)
63.1425	98.21%	47.92%	72.01%

MKSO (First order model)
Surface roughness

$$(\mu\text{m}) = -6.19 + 3.17d + 41.0f + 0.00739v \quad (8)$$

Cutting temperature

$$(^{\circ}\text{C}) = 21.2 + 19.8d - 23f + 0.0353v \quad (9)$$

MOCF (First-order model)
Surface roughness

$$(\mu\text{m}) = -4.84 + 2.2d + 36.1f + 0.00744v \quad (10)$$

Cutting temperature

$$(^{\circ}\text{C}) = 1.9 - 23.5d + 158.3f + 0.1521v \quad (11)$$

MKSO (Second-order model)
Surface roughness

$$(\mu\text{m}) = -8.194 - 9.213d - 135.9f + 0.08908v - 0.000056v^2 + 457.4f^2 + 14.34d^2 + 0.05236vf \quad (12)$$

Cutting temperature

$$(^{\circ}\text{C}) = -202.3 + 131.9d + 1597f + 0.2880v - 0.000207v^2 - 1072f^2 - 154.7d^2 - 2.245vf + 0.366vd \quad (13)$$

MOCF (Second-order model)
Surface roughness

$$(\mu\text{m}) = -9.736 + 0.08820v - 127.4f - 5.101d - 0.000049v^2 + 541.0f^2 + 10.51d^2 - 0.01805vf - 0.02547vd \quad (14)$$

Cutting temperature

$$(^{\circ}\text{C}) = -178.6 + 0.4199v + 424.5f + 186.9d - 0.000129v^2 + 2246f^2 - 152.2d^2 - 1.701vf + 0.1258vd \quad (15)$$

The first-order regression analysis shows a good coefficient of determination values, except for the cutting temperature of MKSO with an R^2 of 28.56%. Meanwhile, the second-order model had a stronger R^2 value that was close to 1. It indicates the model's perfect fit and is statistically significant and acceptable, indicating that the predicted values are extremely close to the experiment data. As a result, the established second-order model predicts that the experimental and anticipated outcomes are highly correlated. This comparison reveals that the established second-order model accurately predicts the expected outcomes and can be implemented safely.

4. Conclusions

Problems in manufacturing are more likely to have multi-objectives than single ones. As a result, this research shows that the Taguchi-GRA technique can be used to solve difficult multi-objective problems. Experiments were carried out using an L_9 orthogonal array, and the findings were analyzed using the Taguchi-GRA approach for optimizing surface roughness, cutting temperature, machine sound level, and machine vibration during the turning of AISI 1525 work material. The Taguchi technique augmented the process, but GRA reduced a complex multiple-response problem to a single unit, known as the grey relational grade. The following findings were derived based on the results obtained.

- i. MKSO extracts were found to be enriched in four compounds: cis-vaccenic acid, hexadecanoic acid, 3-pentadactyl phenol, and squalene.
- ii. MOCF outperformed MKSO by a significant margin in most conditions considered.
- iii. The spindle speed of 0.683 rev/min, feed of 0.617 mm/rev, and depth of cut of 0.620 mm are the optimal characteristics for mango kernel seed oil, while 0.7898 rev/min spindle speed, 0.6483 mm/rev feed, and 0.6373 mm depth of cut are the best specifications for MOCF cutting fluid.
- iv. Spindle speed had the greatest influence on multi-responses in turning operations with both cutting fluids.

Author Contributions: Conceptualization, R.A.K., D.A.F.; methodology, R.A.K. and D.A.F.; software, R.A.K., O.M.I., S.A.A.; validation, O.M.I.; formal analysis, O.M.I., S.A.A.; investigation, R.A.K.; resources, E.T.A., O.M.I., and S.A.A.; data curation, R.A.K., O.M.I., and S.A.A.; writing—original draft preparation, R.A.K.; writing—review and editing, R.A.K., and O.M.I.; visualization, S.A.A. and E.T.A.; supervision, D.A.F. and E.T.A.; project administration, O.M.I., S.A.A. and E.T.A.; funding acquisition, R.A.K., O.M.I. and E.T.A. All authors have read and agreed to the published version of the manuscript.

Funding: This research received no external funding.

Institutional Review Board Statement: Not applicable.

Informed Consent Statement: Not applicable.

Data Availability Statement: Not applicable.

Acknowledgments: Authors acknowledge the University of Ibadan for providing laboratory facilities for the study.

Conflicts of Interest: The authors declare no conflict of interest.

References

1. Oyinbo, S.T.; Ikumapayi, O.M.; Jen, T.C.; Ismail, S.O. Experimental and Numerical prediction of extrusion load at different lubricating conditions of aluminium 6063 alloy in backward cup extrusion. *Eng. Solid Mech.* **2020**, *8*, 119–130. [[CrossRef](#)]
2. Adejuyigbe, S.B.; Ayodeji, S.P. Soybean oil as an alternative to soluble oil in machining mild steel materials. *Niger. J. Pure Appl. Phys.* **2000**, *1*, 17–23. [[CrossRef](#)]
3. Irani, R.A.; Bauer, R.J.; Warkentin, A. A review of cutting fluid application in the grinding process. *Int. J. Mach. Tools Manuf.* **2005**, *45*, 1696–1705. [[CrossRef](#)]
4. Ramana, M.V.; Rao, K.G.; Rao, H.D. Effect of process parameters on surface roughness in turning of titanium alloy under different conditions of lubrication. *Recent Adv. Robot. Aeronaut. Mech. Eng.* **2012**, *3*, 83–91.

5. Singh, T.; Singh, P.; Dureja, J.S.; Dogra, M.; Singh, H.; Bhatti, M.S. A review of near dry machining/minimum quantity lubrication machining of difficult to machine alloys. *Int. J. Mach. Mach. Mater.* **2016**, *18*, 213–251. [[CrossRef](#)]
6. Majak, D.; Olugu, E.U.; Lawal, S.A. Analysis of the effect of sustainable lubricants in the turning of AISI 304 stainless steel. *Procedia Manuf.* **2020**, *43*, 495–502. [[CrossRef](#)]
7. Gunerkar, R.S.; Kuppan, P. Experimental investigation of vegetable oil-based cutting fluid during turning of SS316L. *Int. J. Mech. Eng. Robot. (IJMER)* **2013**, *1*, 46–52.
8. Rapeti, P.; Pasam, V.K.; Gurram, K.M.R.; Revuru, R.S. Performance evaluation of vegetable oil-based nano cutting fluids in machining using a grey relational analysis-A step towards sustainable manufacturing. *J. Clean. Prod.* **2018**, *172*, 2862–2875. [[CrossRef](#)]
9. Shaikh, J.B.; Sidhu, J.S. Experimental investigation and optimization of process parameters in turning of AISI D2 steel using different lubricants. *Int. J. Eng. Adv. Technol.* **2014**, *5*, 189.
10. Kazeem, R.A.; Fadare, D.A.; Abutu, J.; Lawal, S.A.; Adesina, O.S. Performance evaluation of jatropha oil-based cutting fluid in turning AISI 1525 steel alloy. *CIRP J. Manuf. Sci. Technol.* **2020**, *31*, 418–430. [[CrossRef](#)]
11. Ojolo, S.; Amuda, M.; Ogunmola, O.; Ononiwu, C. Experimental determination of the effect of some straight biological oils on cutting force during cylindrical turning. *Matéria (Rio J.)* **2008**, *13*, 650–663. [[CrossRef](#)]
12. Bhowmik, P.; Arora, G.; Pal, N.; Bhardwaj, N. Improving the Surface Texture of Mild Steel using Vegetable Oil as Cutting Fluid. *Int. J. Appl. Eng. Res.* **2014**, *9*, 883–888.
13. Ikumapayi, O.M.; Oyinbo, S.T.; Bodunde, O.P.; Afolalu, S.A.; Okokpujie, I.P.; Akinlabi, E.T. The effects of lubricants on temperature distribution of 6063 aluminium alloy during backward cup extrusion process. *J. Mater. Res. Technol.* **2019**, *8*, 1175–1187. [[CrossRef](#)]
14. Kittiphoom, S.; Sutasinee, S. Mango seed kernel oil and its physicochemical properties. *Int. Food Res. J.* **2013**, *20*, 1145.
15. Puravankara, D.; Boghra, V.; Sharma, R.S. Effect of antioxidant principles isolated from mango (*Mangifera indica* L.) seed kernels on oxidative stability of buffalo ghee (butter-fat). *J. Sci. Food Agric.* **2000**, *80*, 522–526. [[CrossRef](#)]
16. Bhalerao, S.D.; Mulmuley, G.V.; Anathakrishna, S.M.; Potty, V.H. Wash and wastewater management in the food industry. *Fruit Veg. Process. Indian Food Pack.* **1989**, *43*, 5–11.
17. Nzikou, J.M.; Kimbonguila, A.; Matos, L.; Loumouamou, B.; Pambou-Tobi, N.P.G.; Ndangui, C.B.; Abena, A.A.; Silou, T.H.; Scher, J.; Desobry, S. Extraction and characteristics of seed kernel oil from mango (*Mangifera indica*). *Res. J. Environ. Earth Sci.* **2010**, *2*, 31–35.
18. Mohdaly, A.A.; Smetanska, I.; Ramadan, M.F.; Sarhan, M.A.; Mahmoud, A. Antioxidant potential of sesame (*Sesamum indicum*) cake extract in the stabilization of sunflower and soybean oils. *Ind. Crops Prod.* **2011**, *34*, 952–959. [[CrossRef](#)]
19. Firestone, D. *Official Methods and Recommended Practices of the AOCS*; American Oil Chemists' Society: Urbana, IL, USA, 1998; Volume I–II.
20. ASTM D287. *Standard Test Method for API Gravity of Crude Petroleum and Petroleum Products (Hydrometer Method)*; Annual Book of Standards; ASTM International: West Conshohocken, PA, USA, 2012.
21. ASTM D97. *Standard Test Method for Pour Point of Petroleum Products*. *Annual Book of Standards*; Annual Book of Standards; ASTM International: West Conshohocken, PA, USA, 2017.
22. ASTM D2500. *Standard Test Method for Cloud Point of Petroleum Products*; Annual Book of Standards; ASTM International: West Conshohocken, PA, USA, 2005.
23. ASTM D92. *Standard Test Method for Flash and Fire Points by Cleveland Open Cup Tester*; Annual Book of Standards; ASTM International: West Conshohocken, PA, USA, 2002.
24. Muniz, C.A.S.; Dantas, T.N.C.; Moura, E.F.; Neto, A.D.; Gurgel, A. Novel formulations of cutting fluids using naphthenic basic oil. *Braz. J. Pet. Gas* **2009**, *2*, 143–153.
25. Kazeem, R.A.; Fadare, D.A.; Ikumapayi, O.M.; Azeez, T.M.; Adediran, A.A. Development of Bio-Cutting Fluid (*Cirtullus lanatus*) and its Performance Assessment on the Machining of AISI 1525 Steel Using Taguchi Technique and Grey Relational Analysis. *Biointerface Res. Appl. Chem.* **2022**, *12*, 5324–5346.
26. Montgomery, D.C. *Design and Analysis of Experiments*; John Wiley & Sons: Hoboken, NJ, USA, 2017.
27. Lawal, S.A.; Choudhury, I.A.; Nukman, Y. Evaluation of vegetable and mineral oil-in-water emulsion metal cutting fluids in turning AISI 4340 steel with coated carbide tools. *J. Clean. Prod.* **2014**, *66*, 610–618. [[CrossRef](#)]
28. Igwe, O.U.; Okwu, D.E. GC-MS Evaluation of bioactive compounds and antibacterial activity of the oil fraction from the seeds of *Brachystegia eurycoma* Harms. *Asian J. Plant Sci. Res.* **2013**, *3*, 47–54.
29. Smith, T.J. Squalene: Potential chemopreventive agent. *Expert Opin. Investig. Drugs* **2000**, *9*, 1841–1848. [[CrossRef](#)] [[PubMed](#)]
30. Owen, R.W.; Haubner, R.; Würtele, G.; Hull, W.E.; Spiegelhalder, B.; Bartsch, H. Olives and olive oil in cancer prevention. *Eur. J. Cancer Prev.* **2004**, *13*, 319–326. [[CrossRef](#)]
31. Karunanithi, B.; Bogeshwaran, K.; Tripuraneni, M.; Krishna Reddy, S. Extraction of mango seed oil from mango kernel. *Int. J. Eng. Res. Dev.* **2015**, *11*, 32–41.
32. Zhang, J.Z.; Rao, P.N.; Eckman, M. Experimental evaluation of a bio-based cutting fluid using multiple machining characteristics. *Wear* **2012**, *12*, 13–14.
33. Adam, S.A.; Shuaib, N.A.; Hafiezal, M.R.M.; Suhaili, S.N. Study on Surface Roughness and Chip Formation during Milling Operation of Mild Steel Using Vegetable Based Oil as a Lubricant. *Int. J. Eng. Technol. IJET-IJENS* **2013**, *13*, 19–23.

34. Aremu, M.O.; Ibrahim, H.; Bamidele, T.O. Physicochemical characteristics of the oils extracted from some Nigerian plant foods—A review. *Chem. Process. Eng. Res.* **2015**, *32*, 36–52.
35. Kazeem, R.A.; Fadare, D.A.; Ikumapayi, O.M.; Akinlabi, S.A.; Afolalu, S.A.; Akinlabi, E.T. Analysis of the Physicochemical Properties of Some Selected Non-Edible Vegetable Oil-Based Cutting Fluids Using the Design of Experiment (DOE) Approach. *Lubricants* **2022**, *10*, 16. [[CrossRef](#)]
36. Belewu, M.; Adekola, F.; Adebayo, G.; Ameen, O.; Muhammed, N.; Olaniyan, A.; Musa, A. Physico-chemical characteristics of oil and biodiesel from Nigerian and Indian *Jatropha curcas* seeds. *Int. J. Biol. Chem. Sci.* **2010**, *4*, 524–529. [[CrossRef](#)]
37. Panda, A.; Sahoo, A.; Rout, R. Multi-attribute decision making parametric optimization and modeling in hard turning using ceramic insert through grey relational analysis: A case study. *Decis. Sci. Lett.* **2016**, *5*, 581–592. [[CrossRef](#)]
38. Lawal, S.A.; Choudhury, I.A.; Nukman, Y. Application of vegetable oil-based metalworking fluids in machining ferrous metals—A review. *Int. J. Mach. Tools Manuf.* **2012**, *52*, 1–12. [[CrossRef](#)]
39. Mas'ud, F.; Mahendradatta, M.; Laga, A.; Zainal, Z. Optimization of mango seed kernel oil extraction using response surface methodology. *OCL* **2017**, *24*, D503. [[CrossRef](#)]